How to cite: *Angew. Chem. Int. Ed.* **2022,** *61,* e202205348
International Edition: doi.org/10.1002/anie.202205348
German Edition: doi.org/10.1002/ange.202205348

Bioorthogonal Chemistry **Hot Paper**

DFT-Guided Discovery of Ethynyl-Triazolyl-Phosphinates as Modular Electrophiles for Chemoselective Cysteine Bioconjugation and Profiling

Christian E. Stieger, Yerin Park, Mark A. R. de Geus, Dongju Kim, Christiane Huhn, J. Sophia Slenczka, Philipp Ochtrop, Judith M. Müchler, Roderich D. Süssmuth, Johannes Broichhagen, Mu-Hyun Baik, and Christian P. R. Hackenberger**

In memory of Professor Ulf Diederichsen

Abstract: We report the density functional theory (DFT) guided discovery of ethynyl-triazolyl-phosphinates (ETPs) as a new class of electrophilic warheads for cysteine selective bioconjugation. By using Cu^{I}-catalysed azide alkyne cycloaddition (CuAAC) in aqueous buffer, we were able to access a variety of functional electrophilic building blocks, including proteins, from diethynyl-phosphinate. ETP-reagents were used to obtain fluorescent peptide-conjugates for receptor labelling on live cells and a stable and a biologically active antibody-drug-conjugate. Moreover, we were able to incorporate ETP-electrophiles into an azide-containing ubiquitin under native conditions and demonstrate their potential in protein–protein conjugation. Finally, we showcase the excellent cysteine-selectivity of this new class of electrophile in mass spectrometry based, proteome-wide cysteine profiling, underscoring the applicability in homogeneous bioconjugation strategies to connect two complex biomolecules.

Introduction

The chemical functionalization of proteins allows probing and altering their biological function and generating new biotherapeutics, including antibody-drug-conjugates (ADCs).[1,2] In these applications a homogeneous and well-defined conjugate is desired.

One approach to achieve this relies on incorporating unnatural amino acids with distinct bioorthogonal reactivities.[3–5] Alternatively, one can exploit the inherent reactivity of canonical amino acid side chains. Chemoselective modifications of most amino acids in proteins are typically carried out by electrophilic reagents targeting nucleophilic amino acids, especially lysine and cysteine.[2,6–8] The sulfhydryl group of cysteine is a particularly attractive target for bioconjugation due to its low natural abundance and high nucleophilicity under physiological conditions.[9] Maleimides are most frequently employed as electrophiles in cysteine bioconjugation even though the formed thiosuccinimide linkage is susceptible to retro-Michael reaction, which can be problematic for the conjugation of cytotoxic payloads.[10,11] To overcome this problem, several alternative methodologies for cysteine labelling have been developed including vinylsulfonamides,[12] carbonyl acrylic derivatives,[13] hypervalent iodine reagents,[14,15] and organometallic reagents.[16,17] Nonetheless, moderate selectivity or low reactivity under physiological conditions continue to be problematic.[18]

In addition to selectivity and stability concerns, the synthetic accessibility and modularity of the electrophile are important. Whereas peptides can be functionalized with an

[*] C. E. Stieger, Dr. M. A. R. de Geus, C. Huhn, Dr. P. Ochtrop, J. M. Müchler, Dr. J. Broichhagen, Prof. Dr. C. P. R. Hackenberger
Leibniz-Forschungsinstitut für Molekulare Pharmakologie (FMP)
Robert-Rössle-Strasse 10, 13125 Berlin (Germany)
E-mail: hackenbe@fmp-berlin.de

C. E. Stieger, C. Huhn, Dr. P. Ochtrop, J. M. Müchler, Prof. Dr. C. P. R. Hackenberger
Department of Chemistry, Humboldt Universität zu Berlin
Brook-Taylor-Straße 2, 12489 Berlin (Germany)

Y. Park, D. Kim, Prof. Dr. M.-H. Baik
Department of Chemistry, Korea Advanced Institute of Science and Technology (KAIST)
Daejeon 34141 (Republic of Korea)

Y. Park, D. Kim, Prof. Dr. M.-H. Baik
Center for Catalytic Hydrocarbon Functionalizations, Institute for Basic Science (IBS)
Daejeon 34141 (Republic of Korea)
E-mail: mbaik2805@kaist.ac.kr

J. S. Slenczka, Prof. Dr. R. D. Süssmuth
Institut für Chemie, Technische Universität Berlin
Strasse des 17. Juni 124, 10623 Berlin (Germany)

electrophile with ease in organic solvents, aqueous environments pose formidable challenges. Genetically encoding latent bioreactive electrophiles were partially successful,[19] but encoding more reactive electrophiles often results in unspecific side reactions with cytosolic thiols.[20] Therefore, the most common strategy to position a highly reactive electrophile on proteins is the use of bis-electrophilic linkers that can be attached to cysteines or other nucleophilic residues; nevertheless, undesired intramolecular reactions[21] and dimerization are often observed.[22,23] Alternatively, a nucleophilic amino acid can be chemically converted into an electrophile as exemplified by the umpolung of cysteine, tyrosine, and histidine.[24–27]

Another attractive application of electrophiles is in the area of chemoproteomics[28] to label a specific proteome for convenient separation and profiling. For optimal results, the labelling reagents should offer a high target coverage, a uniform modification, excellent amino acid selectivity, and stability of the formed conjugate.[18] To date, this approach is widely applied in elucidating the proteome-wide redox-sensitivity[29] and ligandability of cysteines by electrophilic fragments,[30,31] natural products,[32] or drugs.[33]

As part of our recent effort to establish diethynyl phosphinates as disulfide rebridging reagents for stable antibody modifications, we employed these bisfunctional cysteine-selective electrophiles for the step-wise functionalization of a protein substrate (Scheme 1B).[34] In this protocol, an electrophilic group was installed on a former cysteine sidechain by reaction with diethynyl phosphinate and further reacted with a thiol-containing small-molecule or peptide to generate the desired conjugate. Despite these advances, the incorporation of thiols into small molecules can be synthetically laborious and is accompanied by the inherent problem of disulfide formation. Therefore, we wanted to exploit other modular and synthetically straightforward strategies to incorporate cysteine-selective electrophiles into small molecules, peptides and proteins.

Our current paper describes the discovery of 1,2,3-triazolyl-substituted ethynyl phosphinates (ETPs) as readily accessible, fast, and highly selective thiol-electrophiles (Scheme 1C), guided by density functional theory-based computer models. These molecules can be easily accessed from various azide-containing molecules via copper-catalyzed azide-alkyne cycloaddition (CuAAC) in aqueous buffer. Upon cycloaddition, the electrophiles show a remarkably high reactivity towards cysteine compared to diethynyl-phosphinates and outperform our previously reported phosphonamidate electrophiles (Scheme 1A)[35] in antibody-labelling experiments. We showcase the utility of these reagents in the generation of various biologically relevant peptide-, protein-, and antibody-conjugates. Additionally, we demonstrate that diethynyl-phosphinates can be used to functionalize azide-containing proteins with an ETP-electrophile in aqueous systems and use it for protein-protein conjugation. Finally, we demonstrate the excellent cysteine selectivity of ETP-electrophiles by proteome-wide reactivity profiling.

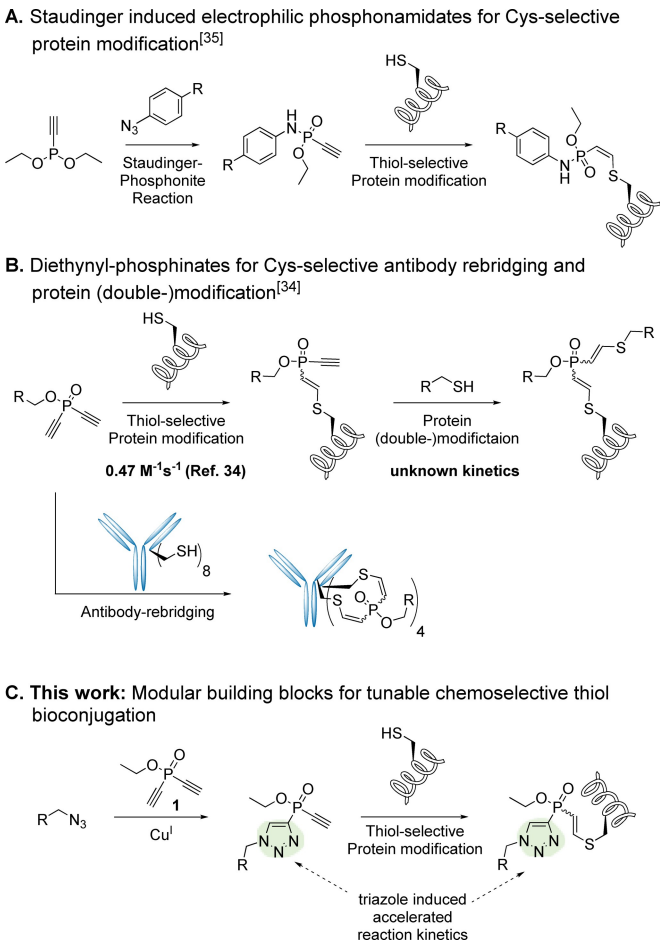

Scheme 1. General concept of unsaturated P^V-electrophiles in Cys-selective protein labelling. A) Electrophilic phosphonamidates, generated via the chemoselective Staudinger-phosphinonite reaction, react selectively with cysteine residues on proteins. B) Diethynyl-phosphinates can react selectively with two distinct thiol-nucleophiles and enable protein double-modification and interchain disulfide rebridging in IgG antibodies. C) Cu^I-click functionalisation of diethynyl-phosphinates generates ETP-reagents that show superior reaction kinetics in cysteine selective protein modification.

Results and Discussion

We started our investigation by determining the kinetic parameters of the second thiol addition to diethynyl-phosphinates (Scheme 1B). Thus, we reacted a small thiol-containing fluorophore (EDANS-SH) with an excess of ethyl diethynyl-phosphinate **1** and obtained thiovinyl-ethynyl phosphinate **2** in good yield (*Z*-isomer, 76 %). **2** was exposed to an equimolar amount of reduced glutathione in an aqueous buffer at pH 8.5[36,37] and we observed smooth conversion to a mixture of the *E*- and *Z*-isomers of the glutathione adduct. The second-order rate constant ($0.29\ M^{-1}s^{-1}$, Figure S5) was found to be slightly lower than the kinetics we reported earlier for the first thiol-addition of the diethynyl-phosphinate ($0.47\ M^{-1}s^{-1}$, Scheme 1B).[34] To increase the reaction speed, we first envisioned to use electron-withdrawing (EWG) alcohol-substituents in **1**, as previously demonstrated for unsaturated

phosphonamidates,[36] however, all attempts to isolate diethynyl-phosphinates bearing EWG alcohol-substituents failed due to rapid hydrolysis of the P–O bond. Prior work from our laboratories showed that density functional theory (DFT) calculations can predict the relative rates of thiol conjugations to the respective P^V-electrophiles.[38] Also, analysis of the molecular orbitals suggested that the key factor in enhancing the reactivity is to stabilize the negatively charged intermediate generated upon the nucleophilic attack of thiolate, where delocalization of the anionic character is achieved through hyperconjugation. The bond P–XEt (X: S, O, and NH) located in an antiperiplanar position to the lone-pair played a decisive role in accepting the electron density. Based on this concept, we interrogated if we can use the accepting ability of new substituents featuring π systems accessible from **1** (i.e., π-acidity) to improve the reactivity. We envisioned that several heterocyclic substituents containing electronegative oxygen and/or nitrogen atoms would be suitable to achieve both, an electron-withdrawing inductive effect and π-conjugation with the lone-pair electrons. Therefore, we focused on the reagents **A**–**E** containing isoxazole (**A**), 1,2,3-triazole (**B** and **C**), 1*H*-pyrazole (**D**) and 3*H*-pyrazole (**E**) substituents and calculated their reaction profiles using DFT. We modelled the reactivity of previously reported **2** by truncating the pendant substituent as a methyl group as compound **F** (Figure 1).

The general scheme of the reaction energy profile for the Michael-addition to the electrophiles **A**–**F** is shown in Figure 1, including ethanethiol (EtSH) as a model nucleophilic reaction component.

In aqueous buffer (e.g. pH 6.5–8.5), EtSH and the corresponding thiolate anion EtS^- are in equilibrium. Since the thiolate is the better nucleophile, we assumed the stepwise deprotonation of EtSH and subsequent nucleophilic attack of EtS^- to form the carbanion intermediate. The calculated reaction barriers ($\Delta G^{\ddagger}$) for respective electrophiles were used to compare the reaction kinetics among them. Calculated $\Delta G^{\ddagger}$ values decrease in the order of 23.3 (**F**) > 20.0 (**C**) ≈ 19.5 (**E**) ≈ 19.0 (**D**) > 18.1 (**A**) ≈ 18.1 kcal mol^{-1} (**B**), suggesting that the newly designed electrophiles **A**–**E** should be much more reactive than **F**. Finally, the intermediate is protonated by water irreversibly to form the final thiol-addition product. The electrophilicity of the series of P^V-reagents can be explained by DFT-calculated partial charges of the reactive terminal carbon atom on the ethynyl group, as atomic charges can be used as a measurement of the electron-withdrawing ability of various functional groups.[39–43] Natural population analysis[44] was conducted to compare the inductive effect posed by the distinctive substituents in electrophiles **A**, **C**, and **F** (Figure 2). The atomic charges (q_C) are correlated to the reaction barriers, being most positive for **A** (−0.092), followed by **C** (−0.108), and most negative for **F** (−0.122).

Along with the partial charges, the frontier molecular orbitals can be used to account for the electrophilicity or nucleophilicity,[42,45–48] where the energy levels of the orbitals affect the efficiency of the bond-forming interaction.[49] Here, the energy of the reactive π* orbital of the P^V-electrophiles is lowest for **A** (−1.65 eV), followed by **C** (−0.93 eV), and highest for **F** (−0.33 eV), in line with the reactivity trend (Figure 2).

We further interrogated how the substituents influence the π-system to enhance the reactivity. Distortion of the P–C≡C bond in the geometry of the transition state (TS) and carbanion intermediate (Int) is characterized by the preference for the sp^2-hybridised lone-pair to be antiperiplanar to the P–R bond (Figure 3a). The optimized TS and intermediate structures of **C** (**C-TS** and **C-Int**) are illustrated in Figure 3a. This structural feature is also found in the previous system, where P–R σ-bonds (R: S, O, and NH) accept electron density via hyperconjugation. Similarly, delocalization of electrons into vacant orbitals related to the P–R bonds is feasible as conceptualized in Figure 3b. The mixing between π-systems of the ethynyl moiety and P–R bond is clearly captured in the LUMO of the electrophiles. The conjugation renders the π^*_y orbital more reactive compared to π^*_z orbital, except in the case of **F**, and ultimately favors the lone-pair electrons to form in that direction. Following the guideline provided by the theoret-

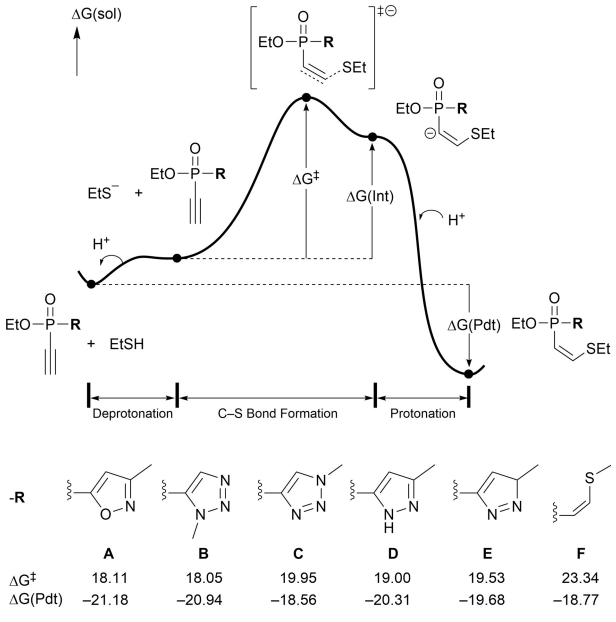

Figure 1. Reaction energy profile of the thiol addition of the proposed reagents **A**–**E** and a model compound **F**. Energies in kcal mol^{-1}, calculated with B3LYP-D3/cc-pVTZ(-f)//B3LYP-D3/6-31G** level of theory.

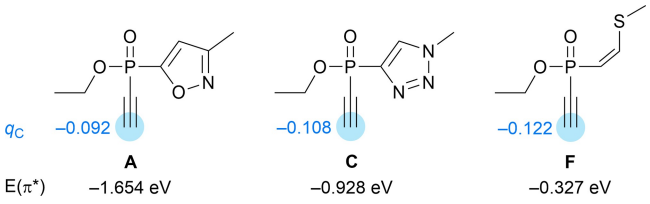

Figure 2. Comparison between electrophiles **A**, **C**, and **F**. q_C: Natural atomic charge at the reactive carbon, $E(\pi^*)$: Energy of the reactive π* orbital of the electrophile. (For more details see Figure S3 and S4).

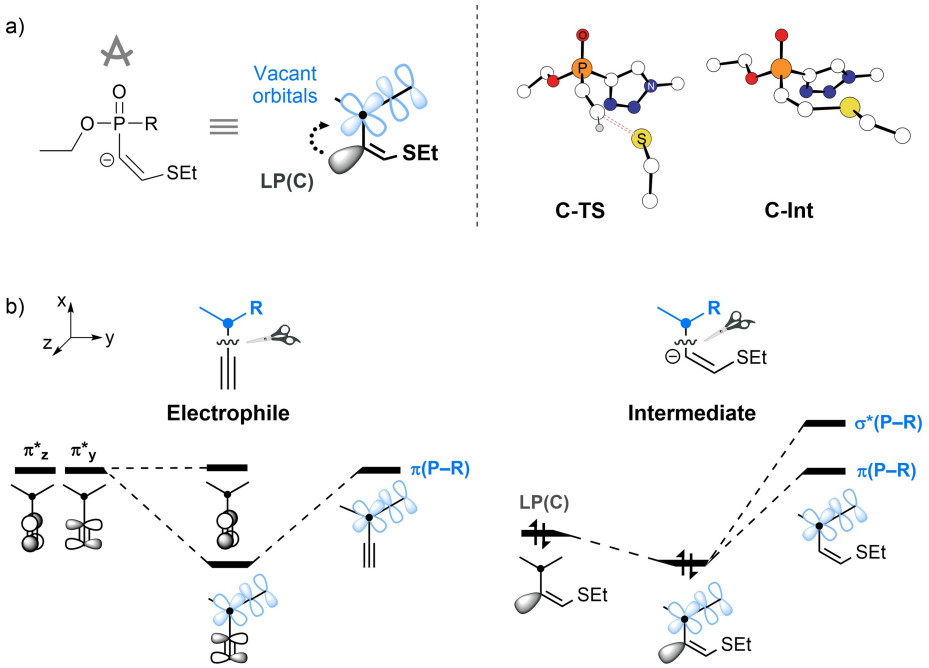

Figure 3. a) The general conformation of transition states and intermediates viewed from the top (left). Geometry of **C-TS** and **C-Int** as representatives (right). b) Conceptualized orbital mixing between two fragments for the LUMO of electrophiles and the HOMO of intermediates. (For the actual molecular orbitals, see Figure S1 and S2).

ical study, we envisioned that 1,2,3-triazole-substituted phosphinate electrophiles could be easily accessed via Cu^{I}-catalyzed azide-alkyne cycloaddition.

Therefore, we investigated the synthesis of ETP-electrophiles starting from EDANS-N_3 and phosphinate **1**. While 1–3 equiv phosphinate in the presence of 10 mol% CuBr resulted mainly in the di-functionalized phosphinate, 5 equiv phosphinate allowed us to obtain the desired mono-functionalized molecule **3** in 85% yield (Scheme 2a). To validate the computational results, we performed kinetic analysis using glutathione as a model thiol as described before. Phosphinate **3** showed accelerated reaction kinetics of 4.61 $M^{-1}s^{-1}$(Figure S5), thus outperforming phosphinate **2** by roughly 15-times, which is in agreement with the DFT-calculated reaction barriers (Scheme 2a). These findings inspired us to synthesize various functionalized ETP-electrophiles (Scheme 2b). Using the described procedure, we were able to generate ETP-reagents bearing fluorophores (**3**, **4**

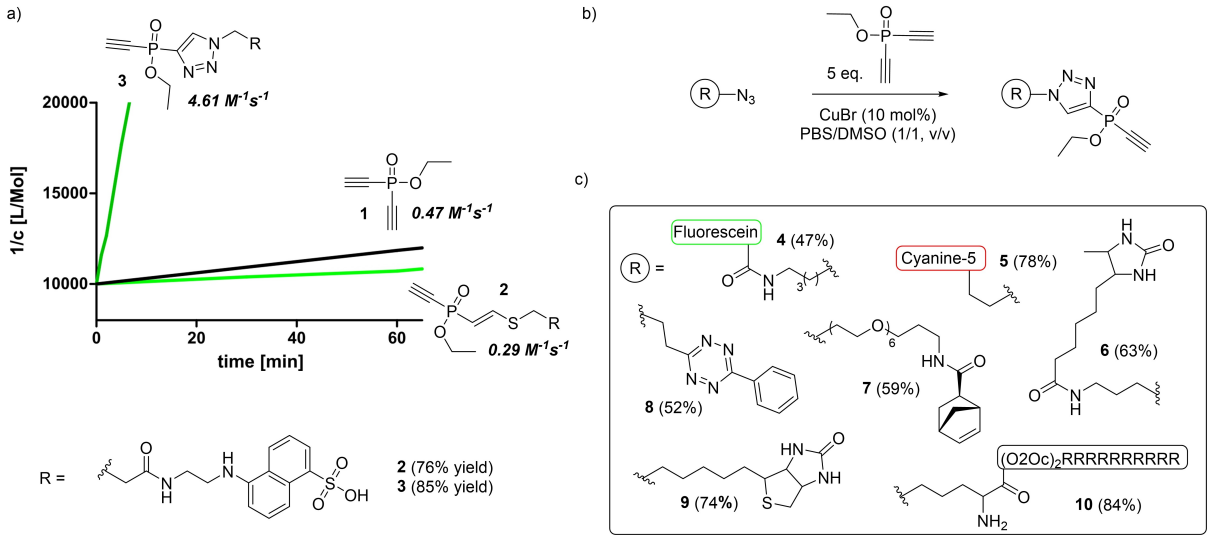

Scheme 2. a) Schematic representation of the experimental thiol addition kinetics of phosphinates **1**–**3** at pH 8.5. b) Synthetic procedure for the generation of functionalized ETP-electrophiles. c) Functional electrophiles obtained via the synthetic procedure depicted in b (values represent isolated yield).

and **5**), affinity-tags (**6** and **9**) or bioorthogonal-click-handles (**7** and **8**) in moderate to good yield. Moreover, we could show that this strategy allows for incorporating an ETP-electrophile into an azide-containing cell-penetrating R_{10}-peptide (**10**) (Scheme 2c).

To probe the applicability of ETP-electrophiles for Cys-selective protein and antibody labelling, we choose the Her2-targeting therapeutic antibody Trastuzumab as a model system. At first, we compared thiovinyl-phosphinate **2** and triazolyl-phosphinate **3**. In brief, Trastuzumab (5 mg mL^{-1} in Tris-buffer pH 8.3) was reduced with 8 equiv TCEP (37 °C, 30 min). Subsequently, 8 equiv of the corresponding phosphinate were added, and the reaction was allowed to proceed overnight at room temperature (Figure 4a). While compound **2** achieved an average labelling of 4.2 fluorophores per antibody, compound **3** reached almost stoichiometric labelling of all free cysteine thiols in the antibody corresponding to a fluorophore-to-antibody-ratio (FAR) of 7.4 (Figure 4b and S6). In a control experiment, in which the antibody was not reduced prior to the reaction with the two phosphinates, no modification could be observed by SDS-PAGE and intact-protein mass spectrometry (MS) (Figure S4b). Also, a larger excess of **3** (100 equiv) did not lead to any antibody-labelling in the absence of a reducing agent (Figure S7).

The observation of almost stoichiometric labelling when using 8 equiv EDANS-ETP led us to explore if this is a general phenomenon. We titrated Trastuzumab with increasing amounts of phosphinates **2** and **3** (Figure 4a). To our delight, we observed full antibody labelling with up to 5 equiv and close to stoichiometric labelling with 6 and 8 equiv for phosphinate **3**. In contrast, compound **2** reached only approximately 50 % labelling for all equivalents after the same time (Figure 4b).

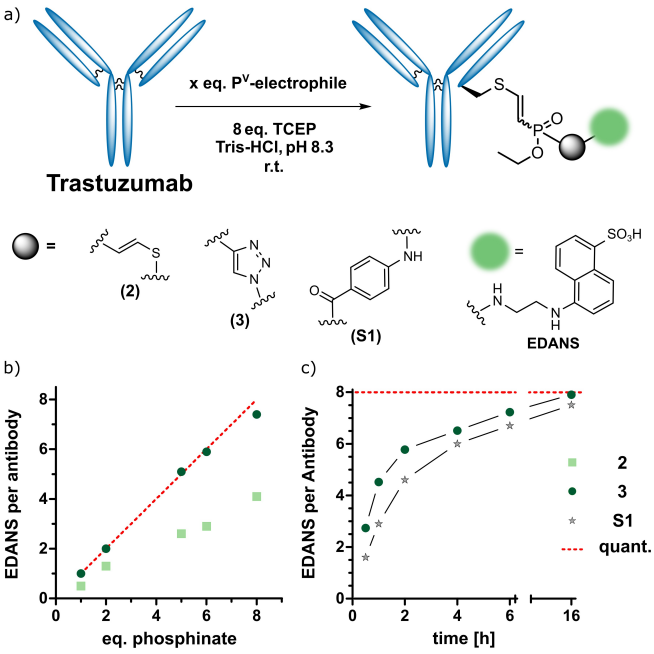

Figure 4. Generation of antibody-fluorophore-conjugates (AFC) using different P^V-electrophiles a) Reaction principle of the simultaneous reduction alkylation reaction using phosphinates **2** and **3** and phosphonamidate **S1** b) Equivalent-screen of the two phosphinates shows close to quantitative labelling with ETP **3** c) Time-course of the antibody labelling reaction using 10 equiv of the corresponding electrophile shows superior reaction kinetics for **3** compared to phosphonamidate **S1**.

Finally, we also compared ethynyl-triazolyl-phosphinates with our previously reported ethynyl-phosphonamidates (PA) in antibody labelling.[35] We performed a time-course experiment, in which reduced Trastuzumab was incubated with 10 equiv of the corresponding P^V-electrophile, monitoring the reaction over 16 h using intact-protein MS. We observed that both the PA- and ETP-reagents reached close to full conversion (FAR 7.5 and 7.9, respectively) after overnight reaction; however, after shorter reaction times phosphinate **3** resulted in a higher degree of functionalization (Figure 4c).

Apart from fast reaction kinetics and cysteine-selectivity, also serum-stability of the linkage is a prerequisite for the successful application in antibody-drug-conjugates to prevent hazardous off-target effects. To test this, we generated an antibody-fluorescein conjugate using phosphinate **4** (see Supporting Information 3.5) and incubated it in human serum for 14 days at 37 °C. Gratifyingly, no significant transfer onto other serum proteins was observed (Figure S8). In addition, we made use of a fluorescence-quenching assay to validate the serum stability of thiol-thiol conjugates formed with diethynyl-phosphinates (see Supporting Information 3.6).[34,35] The quenched FRET-pair **F1** was synthesized from phosphinate **3** and DABCYL-peptide **P2** (38 %, Figure S9a). Incubation of **F1** in a physiologic buffer in the presence of excess small thiols and in human serum did not show any increase in fluorescence signal, indicating excellent stability (Figure S9b).

Encouraged by the straightforward accessibility, high reactivity and stability as cysteine-conjugates we used ETP-electrophiles in the generation of ADCs.

As a payload, we selected Monomethyl-auristatin E (MMAE), a potent anti-mitotic drug commonly used as a cytotoxic payload in the generation of ADCs, which we previously used in thegeneration of phosphonamidate-linked ADCs.[50] After HPLC-purification, the ETP-functionalized drug (**11**) was obtained in 59 % yield after HPLC. (Figure 5a) With the electrophile modified toxin in hand, we started to examine its applicability in antibody labelling. Since the experiments using EDANS-ETP **3** showed that already after 4 hours the majority of the reagent has reacted (Figure 4c), the reactions were terminated and checked after that time. Intact-protein MS revealed that already 5 equiv of the ETP-drug was sufficient to reach an average drug-to-antibody-ratio (DAR) of approximately 4 after the relatively short reaction time. Hence, we did a scale-up of the reaction using 1 mg of Trastuzumab to allow further biological testing. After purification via size-exclusion-chromatography (SEC), the functionalized antibody was obtained in 80 % yield (0.8 mg). Analysis via hydrophobic-interaction-chromatography (HIC) revealed that most of the antibody-molecules are functionalized with 3–6 drug molecules resulting in an average DAR of 4.3 (Figure 5b). The cellular

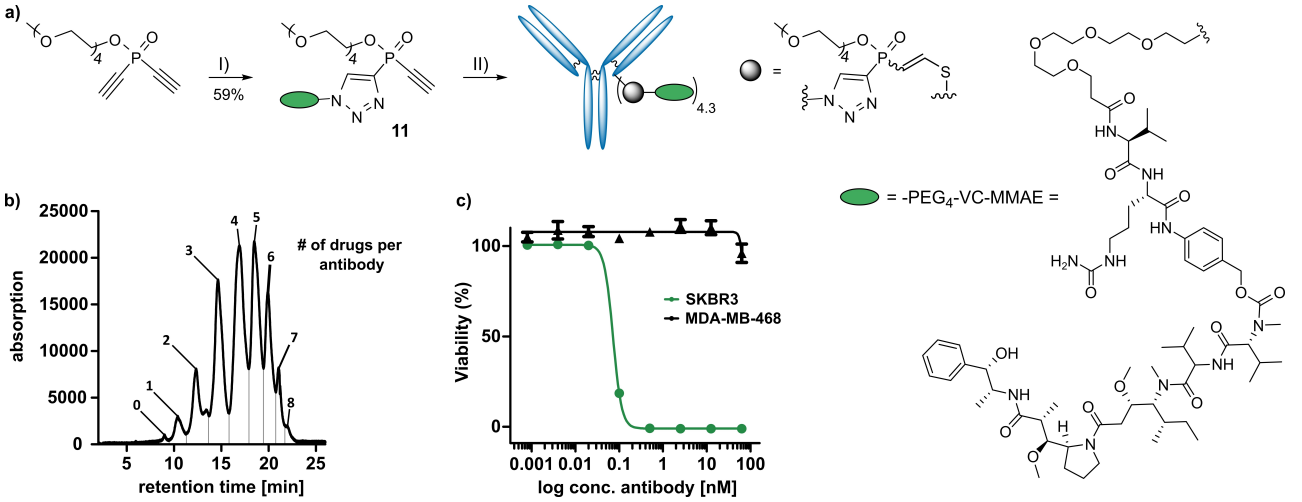

Figure 5. Synthesis and biological evaluation of ETP-derived ADC a) Synthetic route towards the ETP functionalized toxic payload used in the generation of a Trastuzumab based ADC. I) 0.2 equiv N_3-PEG-VC-MMAE, 10 mol% CuBr, PBS/DMSO (2:8, v/v), 0.5 h r.t.; 59% yield. II) 0.2 equiv Trastuzumab (5 mg mL^{-1}), 8 equiv TCEP (with respect to Trastuzumab), Tris-buffer (50 mM, 1 mM EDTA, 100 mM NaCl, pH 8.3), 4 h r.t. b) Hydrophobic-interaction-chromatography of the purified ADC Trastuzumab-**11** c) Concentration dependent cellular cytotoxicity of the generated ADC in Her2+ (SKBR3, green) and Her2- (MDA-MB-468, black) cell lines.

cytotoxicity of our Her2 directed ADC was subsequently evaluated using the Her2$^-$ MDA-MB-468 and the Her2$^+$ SKBR3 cell lines. While the proliferation of the antigen-expressing cell-line could be fully inhibited by Trastuzumab-**11** from concentrations as low as 0.5 nM, antigen-negative cells were only influenced at very high concentrations of the ADC (>100 nM, Figure 5c, S8). These promising results highlight the potential of ETP-reagents as modular building blocks for the generation of efficacious biopharmaceuticals.

Next, we applied these molecules in cysteine-selective peptide modification. As a model peptide we chose Exendin4(9–39) that harbors a serine to cysteine mutation at position 39 (Ex4(9–39)_S39C). This Peptide is a potent antagonist against the glucagon-like peptide-1 receptor (GLP1R),[51] which is a class B G protein-coupled receptor involved in glucose homeostasis and food intake and a blockbuster drug target for the treatment of diabetes (Figure 6a and b).[52,53] Since validated antibodies for its detection remain scarce,[54] we recently endowed Ex4(9–39)_S39C with different fluorophores to obtain **LUXendins**, which specifically label GLP1R in multiple settings.[51,55] The modification of this peptide is particularly challenging because of the three proline residues that are located N-terminal to the C-terminal cysteine. For its derivatization we chose the ETP-functionalized far-red Cy5 fluorophore **5**. After 8 hours of reaction at room temperature the complete consumption of the starting material was observed and the desired peptide-fluorophore conjugate, now termed **P5-LUXendin645** could be isolated in 28% yield after RP-HPLC, as illustrated in Figure 6a. Indeed, **P5-LUXendin645** specifically labelled CHO-K1 cells stably expressing SNAP-GLP1R[56] as highlighted by widefield microscopy with no indication of inferior performance over its stablemate LUXendin645 (Figure 6c). SNAP-tag labelling was used to unambiguously demonstrate **P5-LUXendin645**s specificity

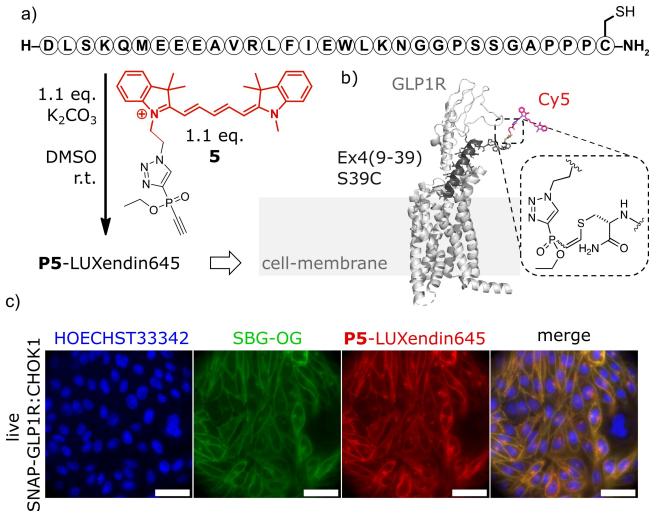

Figure 6. Synthesis and application of a P5-linked LUXendin645. a) Primary sequence of the LUXendin backbone Ex4(9–39)_S39C is endowed with Cy5 electrophile **5** to yield **P5-LUXendin645**. b) Schematic representation of **P5-LUXendin645** bound to GLP1R highlighting the linker chemistry. c) Microscopy of live SNAP-GLP1R:CHO-K1 cells using far-red **P5-LUXendin645** in red (Hoechst33342 in blue, SBG-OG for cell surface SNAP-tag labelling in green). Scale bar = 40 µm.

on SNAP-GLP1R by using a cell impermeable, Oregon Green containing substrate SBG-OG,[57] while non-transfected cells served as controls and remained unstained upon application of P5-Luxendin645 (Figure S11).

In addition to the generation of small-molecule- and peptide-based ETP-electrophiles, we were curious if one can expand this strategy to functionalize azide-containing proteins and apply them in protein-protein conjugations. For a proof of principle, we chose ubiquitin (Ub) as a model protein. The attachment of Ub onto a target protein, also

referred to as ubiquitination, is a reversible post-translational modification, regulating a multitude of cellular processes including protein degradation and DNA repair.[58] Earlier studies have demonstrated, that chemically synthesized poly-ubiquitins with different conjugation sites are a valuable tool to study their biological function.[59] We reported previously the incorporation of electrophilic vinylphosphonothiolates into Ub and the subsequent application in artificial protein-ubiquitinylation.[37] This approach comes with the drawbacks that anhydrous DMSO supplemented with TFA has to be used as a solvent, and subsequent HPLC-purification is required. In contrast as demonstrated in this paper, the incorporation of the ETP-electrophile can be achieved in physiological buffers with only a small amount of organic co-solvents. Moreover, we envisioned that the enhanced reactivity of the ETP-electrophile compared to the phosphonothiolate results in superior protein-protein conjugation. To obtain an azide-containing protein, we used an approach developed by Schneider et al. that allows to introduce azidohomoalanine (Aha) into Ub via selective pressure incorporation.[60] Following this procedure, we expressed the two Ub-mutants UbK48Aha and UbK63Aha for subsequent modification with phosphinate **1** (Figure 7a and Supporting Information 3.9). Compared to the small-molecule experiments, we slightly adapted our CuAAC-protocol (see Supporting Information 3.10). After 5 h reaction time, we observed full conversion of the Aha-mutants via intact-protein MS. Excess copper, ligand, and phosphinate were removed via dialysis against PBS supplemented with 5 mM EDTA for 16 h, followed by size exclusion chromatography (SEC) to obtain ETP-modified **UbK63-ETP** and **UbK48-ETP** in 74 % and 62 % yield, respectively (Figure 7b). Next, we wished to leverage these protein-electrophiles in protein-protein conjugation. Therefore, we subjected both **UbK63-ETP** and **UbK48-ETP** to the bioconjugation with an UbG76C mutant. The reactions were carried out in Tris-buffer at pH 8 and monitored via intact-protein-MS and SDS-PAGE (Figure 7c and d and S12). The starting material was fully consumed after 6 h reaction time, and the corresponding Ub-dimers (**12** and **13**) were purified via SEC and isolated in 58 % and 47 % yield.

To verify the linkage and cysteine-selectivity, the purified dimers were digested using trypsin and analyzed via bottom-up proteomics. The use of both conventional and dedicated cross-linking proteomics software allowed verifying the correct linkage sites, with no detectable side-reactivity (Figure 7e and S13).[61,62] Furthermore, the protease resistance of the linkage-specifically synthesized ubiquitin dimers against deubiquitinating enzymes (DUBs) was investigated. While the DUB USP2 was able to cleave K48-linked wild-type diubiquitin completely, no degradation of our synthetic analogue **12** was observed (Figure 7f).

Having demonstrated the utility of ETP-reagents for cysteine selective protein modification, we were intrigued to probe this compound-class in proteome-wide cysteine labeling and profiling in whole-cell lysates. To test this, HEK293 cell-lysate (1 mg mL^{-1} in PBS pH 7.4) was treated with increasing amounts of phosphinate **4** for 45 minutes at room temperature before analysis via SDS-PAGE and in-gel fluorescence (Figure 8a). Coomassie staining was used to control for equal loading. We observed concentration-dependent labeling of the lysate and already at 30 µM **4** a decent fluorescent signal was observed (Figure 8b).

To identify the sites of labelling, we made use of desthiobiotin-ETP **6** and adapted a workflow that allows for the unbiased analysis of electrophile selectivity on proteome scale, recently developed by Zanon et al.[18] (Figure 8c). In brief, HEK293-lysate (1 mg mL^{-1}, PBS pH 8.3) was treated with 200 µM of phosphinate **6** for 45 minutes at room temperature. Afterward, the proteins were precipitated using ice-cold acetone and enriched using streptavidin beads. After tryptic digestion and elution of the labeled peptides, the samples were analyzed by high-resolution liquid-chromatography couple tandem mass spectrometry (LC-MS/MS). To identify the modification mass, we performed an open search in MS-Fragger using previously optimized settings.[18,63] We were pleased to confirm that the most prominent modification in all three replicates corresponds to the expected mass of an alkylation with phosphinate **6** (Δm_{exp}, 27137 peptide spectrum matches (PSMs)). Moreover, the modification-mass plus oxidation (Δm_{Ox}, 1747 PSMs), formylation (Δm_{f}, 2005 PSMs), and carbamidometh-

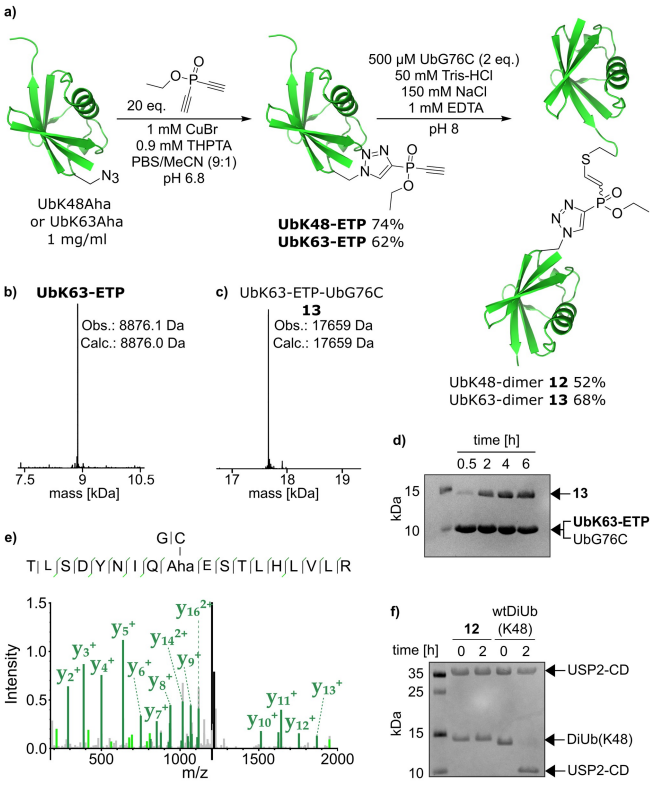

Figure 7. a) Synthetic strategy to obtain electrophilic ubiquitin from site-selectively installed K→Aha mutants. b) and c) Intact protein-MS of the ETP-functionalized **UbK63-ETP** (b) and the artificial Ub-dimer **13** (c). d) Time course of the conjugation of **UbK63-ETP** to UbG76C monitored by SDS-Page. e) MS/MS-spectrum identifying the linkage-site of **13**. f) SDS-PAGE analysis of Ub-dimer **12** incubated with USP2-CD.

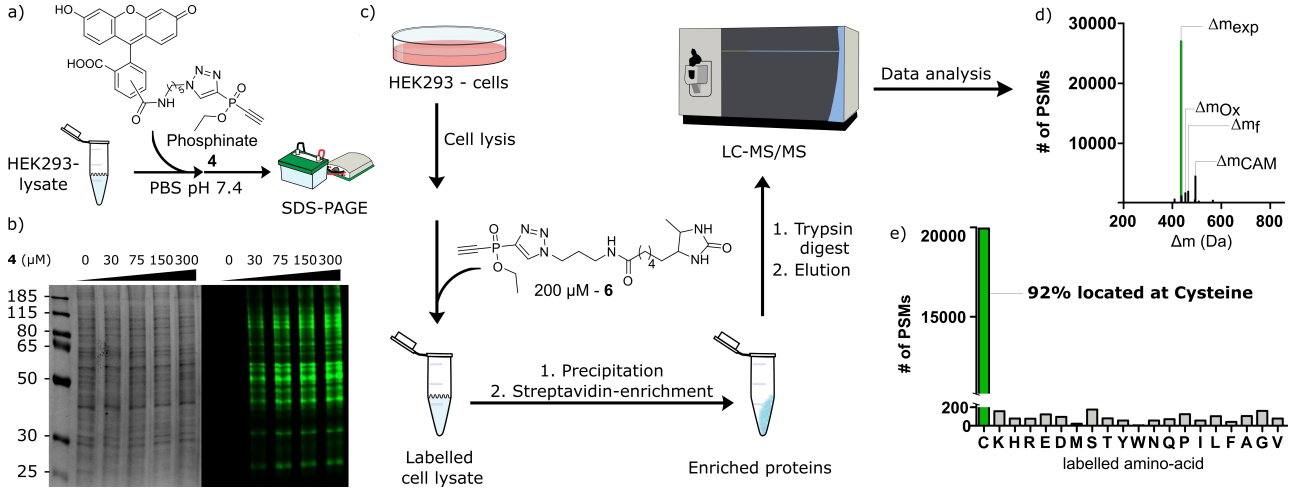

Figure 8. Investigation of proteome-wide cysteine reactivity of ETP-electrophiles. a) Workflow for the labelling of whole-cell lysate using the fluorescent phosphinate **4** and subsequent analysis. b) SDS-PAGE analysis of cell lysate treated with increasing electrophile concentration. c) Illustration of the workflow used for the unbiased analysis of electrophile selectivity via MS-based proteomics. d) Histogram of the modifications detected in MS-Fragger open search across three replicates. Δm of phosphinate **6** is highlighted in green. ox = oxidation (+15.99 Da), f = formylation (+27.99 Da), CAM = carbamidomethylation (+57.02 Da) e) Abundance of identified modification sites when using Δm_{exp} as offset-mass. # of PSMs represents the sum of three independent replicates.

ylation (Δm_{CAM}, 4546 PSMs) were detected as well (Figure 8d).

After identifying the modification mass, our next step was to analyze the amino acid selectivity. Therefore, we performed an offset-mass search using Δm_{exp} as the modification mass. In this search, every amino acid is considered a potential modification site, allowing for an unbiased investigation.

The obtained results were filtered to contain only PSMs within 1% peptide level false discovery rate (FDR), to ensure good data quality. Moreover, only spectra where MS-Fragger was able to assign a single modification site were considered in our analysis. Out of 22102 spectra that matched the aforementioned criteria, 20429 (92%) were located at a cysteine residue (Figure 8e). The remaining spectra were distributed among all other 19 proteinogenic amino acids, with none of them reaching more than 150 spectral matches (<0.7%). Taking a closer look at the results, we found that out of the 1673 spectra that were not localized to a cysteine, 817 are assigned to an amino acid residue adjacent to a cysteine. Unambiguous site-localization is often difficult when MS/MS spectra do not contain enough fragment peaks. To account for this uncertainty, we applied a delta-score >1 (the score-difference between best and second-best modification site). From the remaining spectra (19595 PSMs), 95% were found to be modified on a cysteine (Figure S14). These findings further underline the excellent cysteine-selectivity of ETP-electrophiles. Finally, we performed a conventional search using MS Amanda[61] applying the obtained parameters for desthiobiotin-ETP (modification-mass: 438.2136; modification-site: Cys) as a variable modification (see Supporting Information 2.11.2 for details). In total, 8661 unique labelled cysteine sites derived from 3978 proteins could be identified from three independent replicates. Interestingly we found that even at a lower cell lysate concentration along with a lower total proteomic input (0.1 mg mL^{-1}, 50 μg total), 7023 unique cysteine sites could still be detected (Figure S15).

Conclusion

This work has introduced ethynyl-triazolyl-phosphinates as modular, highly cysteine-selective electrophiles for protein- and antibody labelling. The discovery of this compound class was enabled using DFT-calculations that successfully predicted superior thiol-addition kinetics compared to diethynyl- or thiovinyl-phosphinates. We demonstrated that various functional payloads can be easily equipped with ETP-electrophiles by a straightforward CuAAC-protocol, which offers the unique opportunity for the site-specific incorporation of highly reactive electrophiles into proteins. The potential of this chemistry in the generation of functional bioconjugates was further highlighted by the generation of an ADC with cell-specific toxicity and fluorescent peptides specifically targeting cell-surface receptors. Moreover, the cysteine-selectivity was demonstrated on a proteome scale by probing accessible cysteine residues in cell-lysate, followed by their analysis using bottom-up proteomics. Given the easy accessibility, fast reaction kinetics and excellent stability as bioconjugates, we anticipate that ETP-reagents will find widespread application as electrophilic chemical probes and in the generation of highly valuable protein-conjugates and furnish the development of next-generation biopharmaceuticals.

The mass spectrometry proteomics data have been deposited to the ProteomeXchange Consortium via the PRIDE partner repository[64] with the dataset identifier PXD033004.[65]

Acknowledgements

We are grateful to I. Kretzschmer and R. Volkmer for SPPS, R. Birke for microscopic assistance, K. K.-Hassanin for expressing Ub-Aha mutants, B. Kindt for technical assistance and M. Holly-Nadler for assistance with LC-MS/MS measurements. We thank Dr. B. Jones (Imperial London) for providing the stable SNAP-GLP1R:CHO-K1 cell line and Dr. M.-A. Kasper (Tubulis) for Cy5-N_3. This work was supported by grants from the Deutsche Forschungsgemeinschaft (DFG, SPP1623 HA 4468/10-1 and RTG2473 "Bioactive Peptides" Projektnummer 392923329), the Leibniz Society (SAW-2018-FMP-4-P5label, T18/2017) and the Einstein Foundation Berlin (Leibniz-Humboldt Professorship). The computational studies were supported by the Institute for Basic Science in Korea (IBS-R10-A1). C.E.S. is supported by a PhD-fellowship of the Studienstiftung des Deutschen Volkes and M.A.R.deG. by a PostDoc-fellowship of the Alexander von Humboldt foundation. Open Access funding enabled and organized by Projekt DEAL.

Conflict of Interest

The chemistry described in this manuscript is part of a patent application (Appl. Number: EP21170097.6) by C.E.S., P.O. and C.P.R.H. J.B. has a licensing agreement with Celtarys Research for LUXendin distribution.

Data Availability Statement

The mass spectrometry proteomics data have been deposited to the ProteomeXchange Consortium via the PRIDE partner repository with the dataset identifier PXD033004 (C. E. Stieger, C. P. R. Hackenberger, 2022, Ethynyl-1,2,3-triazolyl-phosphinate based electrophiles for cysteine labelling, PRIDE, PXD033004).

Keywords: Antibody-Drug-Conjugates · Bioconjugation · Cysteine Profiling · Protein-Based Electrophiles · Protein–Protein Conjugation

[1] A. Beck, L. Goetsch, C. Dumontet, N. Corvaïa, *Nat. Rev. Drug Discovery* **2017**, *16*, 315–337.
[2] E. A. Hoyt, P. M. S. D. Cal, B. L. Oliveira, G. J. L. Bernardes, *Nat. Rev. Chem.* **2019**, *3*, 147–171.
[3] J. L. Seitchik, J. C. Peeler, M. T. Taylor, M. L. Blackman, T. W. Rhoads, R. B. Cooley, C. Refakis, J. M. Fox, R. A. Mehl, *J. Am. Chem. Soc.* **2012**, *134*, 2898–2901.
[4] K. Lang, L. Davis, J. Torres-Kolbus, C. Chou, A. Deiters, J. W. Chin, *Nat. Chem.* **2012**, *4*, 298–304.
[5] R. D. Row, H.-W. Shih, A. T. Alexander, R. A. Mehl, J. A. Prescher, *J. Am. Chem. Soc.* **2017**, *139*, 7370–7375.
[6] P. Ochtrop, C. P. R. Hackenberger, *Curr. Opin. Chem. Biol.* **2020**, *58*, 28–36.
[7] N. C. Reddy, M. Kumar, R. Molla, V. Rai, *Org. Biomol. Chem.* **2020**, *18*, 4669–4691.
[8] S. Sakamoto, I. Hamachi, *Anal. Sci.* **2019**, *35*, 5–27.
[9] A. Moura, M. A. Savageau, R. Alves, *PLoS One* **2013**, *8*, e77319.
[10] B. Q. Shen, K. Xu, L. Liu, H. Raab, S. Bhakta, M. Kenrick, K. L. Parsons-Reponte, J. Tien, S. F. Yu, E. Mai, D. Li, J. Tibbitts, J. Baudys, O. M. Saad, S. J. Scales, P. J. McDonald, P. E. Hass, C. Eigenbrot, T. Nguyen, W. A. Solis, R. N. Fuji, K. M. Flagella, D. Patel, S. D. Spencer, L. A. Khawli, A. Ebens, W. L. Wong, R. Vandlen, S. Kaur, M. X. Sliwkowski, R. H. Scheller, P. Polakis, J. R. Junutula, *Nat. Biotechnol.* **2012**, *30*, 184–189.
[11] C. Wei, G. Zhang, T. Clark, F. Barletta, L. N. Tumey, B. Rago, S. Hansel, X. Han, *Anal. Chem.* **2016**, *88*, 4979–4986.
[12] R. Huang, Z. Li, Y. Sheng, J. Yu, Y. Wu, Y. Zhan, H. Chen, B. Jiang, *Org. Lett.* **2018**, *20*, 6526–6529.
[13] B. Bernardim, P. M. S. D. Cal, M. J. Matos, B. L. Oliveira, N. Martínez-Saéz, I. S. Albuquerque, E. Perkins, F. Corzana, A. C. B. Burtoloso, G. Jiménez-Osés, G. J. L. Bernardes, *Nat. Commun.* **2016**, *7*, 13128.
[14] R. Tessier, J. Ceballos, N. Guidotti, R. Simonet-Davin, B. Fierz, J. Waser, *Chem* **2019**, *5*, 2243–2263.
[15] S. A. Byrne, M. J. Bedding, L. Corcilius, D. J. Ford, Y. Zhong, C. Franck, M. Larance, J. P. Mackay, R. J. Payne, *Chem. Sci.* **2021**, *12*, 14159–14166.
[16] E. V. Vinogradova, C. Zhang, A. M. Spokoyny, B. L. Pentelute, S. L. Buchwald, *Nature* **2015**, *526*, 687–691.
[17] M. S. Messina, J. M. Stauber, M. A. Waddington, A. L. Rheingold, H. D. Maynard, A. M. Spokoyny, *J. Am. Chem. Soc.* **2018**, *140*, 7065–7069.
[18] P. R. A. Zanon, F. Yu, P. Z. Musacchio, L. Lewald, M. Zollo, K. Krauskopf, D. Mrdović, P. Raunft, T. E. Maher, M. Cigler, C. J. Chang, K. Lang, F. D. Toste, A. I. Nesvizhskii, S. M. Hacker, *ChemRxiv* **2021**, https://doi.org/10.26434/chemrxiv.14186561.
[19] T.-A. Nguyen, M. Cigler, K. Lang, *Angew. Chem. Int. Ed.* **2018**, *57*, 14350–14361; *Angew. Chem.* **2018**, *130*, 14548–14559.
[20] J. L. Furman, M. Kang, S. Choi, Y. Cao, E. D. Wold, S. B. Sun, V. V. Smider, P. G. Schultz, C. H. Kim, *J. Am. Chem. Soc.* **2014**, *136*, 8411–8417.
[21] V. Laserna, A. Istrate, K. Kafuta, T. A. Hakala, T. P. J. Knowles, M. Alcarazo, G. J. L. Bernardes, *Bioconjugate Chem.* **2021**, *32*, 1570–1575.
[22] M.-A. Kasper, L. Lassak, A. M. Vogl, I. Mai, J. Helma, D. Schumacher, C. P. R. Hackenberger, *Eur. J. Org. Chem.* **2022**, e202101389.
[23] L. Xu, S. L. Kuan, T. Weil, *Angew. Chem. Int. Ed.* **2021**, *60*, 13757–13777; *Angew. Chem.* **2021**, *133*, 13874–13894.
[24] M. J. Lobba, C. Fellmann, A. M. Marmelstein, J. C. Maza, E. N. Kissman, S. A. Robinson, B. T. Staahl, C. Urnes, R. J. Lew, C. S. Mogilevsky, J. A. Doudna, M. B. Francis, *ACS Cent. Sci.* **2020**, *6*, 1564–1571.
[25] K. Nakane, S. Sato, T. Niwa, M. Tsushima, S. Tomoshige, H. Taguchi, M. Ishikawa, H. Nakamura, *J. Am. Chem. Soc.* **2021**, *143*, 7726–7731.
[26] L.-Q. Wan, X. Zhang, Y. Zou, R. Shi, J.-G. Cao, S.-Y. Xu, L.-F. Deng, L. Zhou, Y. Gong, X. Shu, G. Y. Lee, H. Ren, L. Dai, S. Qi, K. N. Houk, D. Niu, *J. Am. Chem. Soc.* **2021**, *143*, 11919–11926.
[27] A. M. White, I. R. Palombi, L. R. Malins, *Chem. Sci.* **2022**, *13*, 2809–2823.
[28] A. J. Maurais, E. Weerapana, *Curr. Opin. Chem. Biol.* **2019**, *50*, 29–36.
[29] E. Weerapana, C. Wang, G. M. Simon, F. Richter, S. Khare, M. B. D. Dillon, D. A. Bachovchin, K. Mowen, D. Baker, B. F. Cravatt, *Nature* **2010**, *468*, 790–795.
[30] K. M. Backus, B. E. Correia, K. M. Lum, S. Forli, B. D. Horning, G. E. González-Páez, S. Chatterjee, B. R. Lanning,

J. R. Teijaro, A. J. Olson, D. W. Wolan, B. F. Cravatt, *Nature* **2016**, *534*, 570–574.
[31] P. R. A. Zanon, L. Lewald, S. M. Hacker, *Angew. Chem. Int. Ed.* **2020**, *59*, 2829–2836; *Angew. Chem.* **2020**, *132*, 2851–2858.
[32] D. Abegg, R. Frei, L. Cerato, D. Prasad Hari, C. Wang, J. Waser, A. Adibekian, *Angew. Chem. Int. Ed.* **2015**, *54*, 10852–10857; *Angew. Chem.* **2015**, *127*, 11002–11007.
[33] M. Kuljanin, D. C. Mitchell, D. K. Schweppe, A. S. Gikandi, D. P. Nusinow, N. J. Bulloch, E. V. Vinogradova, D. L. Wilson, E. T. Kool, J. D. Mancias, B. F. Cravatt, S. P. Gygi, *Nat. Biotechnol.* **2021**, *39*, 630–641.
[34] C. E. Stieger, L. Franz, F. Körlin, C. P. R. Hackenberger, *Angew. Chem. Int. Ed.* **2021**, *60*, 15359–15364; *Angew. Chem.* **2021**, *133*, 15487–15492.
[35] M.-A. Kasper, M. Glanz, A. Stengl, M. Penkert, S. Klenk, T. Sauer, D. Schumacher, J. Helma, E. Krause, M. C. Cardoso, H. Leonhardt, C. P. R. Hackenberger, *Angew. Chem. Int. Ed.* **2019**, *58*, 11625–11630; *Angew. Chem.* **2019**, *131*, 11751–11756.
[36] M.-A. Kasper, M. Glanz, A. Oder, P. Schmieder, J. P. Von Kries, C. P. R. Hackenberger, *Chem. Sci.* **2019**, *10*, 6322–6329.
[37] A. L. Baumann, S. Schwagerus, K. Broi, K. Kemnitz-Hassanin, C. E. Stieger, N. Trieloff, P. Schmieder, C. P. R. Hackenberger, *J. Am. Chem. Soc.* **2020**, *142*, 9544–9552.
[38] Y. Park, A. L. Baumann, H. Moon, S. Byrne, M.-A. Kasper, S. Hwang, H. Sun, M.-H. Baik, C. P. R. Hackenberger, *Chem. Sci.* **2021**, *12*, 8141–8148.
[39] S. L. Dixon, P. C. Jurs, *J. Comput. Chem.* **1993**, *14*, 1460–1467.
[40] C. A. Hollingsworth, P. G. Seybold, C. M. Hadad, *Int. J. Quantum Chem.* **2002**, *90*, 1396–1403.
[41] K. C. Gross, P. G. Seybold, C. M. Hadad, *Int. J. Quantum Chem.* **2002**, *90*, 445–458.
[42] C. Wang, Y. Fu, Q.-X. Guo, L. Liu, *Chem. Eur. J.* **2010**, *16*, 2586–2598.
[43] S. Liu, C. Rong, T. Lu, *J. Phys. Chem. A* **2014**, *118*, 3698–3704.
[44] A. E. Reed, R. B. Weinstock, F. Weinhold, *J. Chem. Phys.* **1985**, *83*, 735–746.
[45] K. N. Houk, *Acc. Chem. Res.* **1975**, *8*, 361–369.
[46] L.-G. Zhuo, W. Liao, Z.-X. Yu, *Asian J. Org. Chem.* **2012**, *1*, 336–345.
[47] Z. Demircioğlu, Ç. A. Kaştaş, O. Büyükgüngör, *J. Mol. Struct.* **2015**, *1091*, 183–195.
[48] J. Fleming, *Frontier Orbitals and Organic Chemical Reactions*, Wiley, London, **1976**.
[49] K. Fukui, *Science* **1982**, *218*, 747–754.
[50] M.-A. Kasper, A. Stengl, P. Ochtrop, M. Gerlach, T. Stoschek, D. Schumacher, J. Helma, M. Penkert, E. Krause, H. Leonhardt, C. P. R. Hackenberger, *Angew. Chem. Int. Ed.* **2019**, *58*, 11631–11636; *Angew. Chem.* **2019**, *131*, 11757–11762.
[51] J. Ast, A. Arvaniti, N. H. F. Fine, D. Nasteska, F. B. Ashford, Z. Stamataki, Z. Koszegi, A. Bacon, B. J. Jones, M. A. Lucey, S. Sasaki, D. I. Brierley, B. Hastoy, A. Tomas, G. D'Agostino, F. Reimann, F. C. Lynn, C. A. Reissaus, A. K. Linnemann, E. D'Este, D. Calebiro, S. Trapp, K. Johnsson, T. Podewin, J. Broichhagen, D. J. Hodson, *Nat. Commun.* **2020**, *11*, 467.
[52] L. L. Baggio, D. J. Drucker, *Gastroenterology* **2007**, *132*, 2131–2157.
[53] J. E. Campbell, D. J. Drucker, *Cell Metab.* **2013**, *17*, 819–837.
[54] J. Ast, J. Broichhagen, D. J. Hodson, *EBioMedicine* **2021**, *74*, 103739.
[55] J. Ast, A. N. Novak, T. Podewin, N. H. F. Fine, B. Jones, A. Tomas, R. Birke, K. Roßmann, B. Mathes, J. Eichhorst, M. Lehmann, A. K. Linnemann, D. J. Hodson, J. Broichhagen, *JACS Au* **2022**, *2*, 1007–1017.
[56] B. J. Jones, R. Scopelliti, A. Tomas, S. R. Bloom, D. J. Hodson, J. Broichhagen, *ChemistryOpen* **2017**, *6*, 501–505.
[57] P. Poc, V. A. Gutzeit, J. Ast, J. Lee, B. J. Jones, E. D'Este, B. Mathes, M. Lehmann, D. J. Hodson, J. Levitz, J. Broichhagen, *Chem. Sci.* **2020**, *11*, 7871–7883.
[58] K. N. Swatek, D. Komander, *Cell Res.* **2016**, *26*, 399–422.
[59] X. Sui, Y. Wang, Y. X. Du, L. J. Liang, Q. Zheng, Y. M. Li, L. Liu, *Chem. Sci.* **2020**, *11*, 12633–12646.
[60] T. Schneider, D. Schneider, D. Rösner, S. Malhotra, F. Mortensen, T. U. Mayer, M. Scheffner, A. Marx, *Angew. Chem. Int. Ed.* **2014**, *53*, 12925–12929; *Angew. Chem.* **2014**, *126*, 13139–13143.
[61] V. Dorfer, P. Pichler, T. Stranzl, J. Stadlmann, T. Taus, S. Winkler, K. Mechtler, *J. Proteome Res.* **2014**, *13*, 3679–3684.
[62] M. Götze, J. Pettelkau, S. Schaks, K. Bosse, C. H. Ihling, F. Krauth, R. Fritzsche, U. Kühn, A. Sinz, *J. Am. Soc. Mass Spectrom.* **2012**, *23*, 76–87.
[63] F. Yu, G. C. Teo, A. T. Kong, S. E. Haynes, D. M. Avtonomov, D. J. Geiszler, A. I. Nesvizhskii, *Nat. Commun.* **2020**, *11*, 4065.
[64] Y. Perez-Riverol, J. Bai, C. Bandla, D. García-Seisdedos, S. Hewapathirana, S. Kamatchinathan, D. J. Kundu, A. Prakash, A. Frericks-Zipper, M. Eisenacher, M. Walzer, S. Wang, A. Brazma, J. A. Vizcaíno, *Nucleic Acids Res.* **2022**, *50*, D543–D552.
[65] C. E. Stieger, C. P. R. Hackenberger, **2022**, Ethynyl-1,2,3-triazolyl-phosphinate based electrophiles for cysteine labelling, PRIDE, PXD033004.

Manuscript received: April 12, 2022
Accepted manuscript online: July 6, 2022
Version of record online: August 22, 2022